

Probing lattice distortions in mixed $\text{CH}_3\text{I}_{1-c}\text{Br}_c$ by methyl rotational tunneling

M. Prager^{a)}

Institut für Festkörperforschung, Forschungszentrum Jülich D-52425 Jülich, Germany

(Received 19 August 2003; accepted 30 October 2003)

Methyl iodide alloyed with methyl bromide is studied for low methyl bromide concentrations $c \leq 0.3$ by rotational tunneling spectroscopy with neutrons. The appearance of three tunneling bands, their shift with respect to the pure materials and their broadening is explained semiquantitatively on the basis of the crystal structure and global and local changes of interatomic distances based on the r -dependence of intermolecular interactions. Besides the overall reduction of the lattice parameter local free volume around guest molecules is important. A local relaxation of the atomic position by 1.3% towards guest molecules is found. © 2004 American Institute of Physics.
[DOI: 10.1063/1.1635817]

I. INTRODUCTION

The simpler a molecular crystal the more a quantitative analysis of experimental data is possible. The most fundamental molecular crystals are hydrogen¹ and methane.² Among the next “simple” materials is water³ and the methyl halides.⁴ The spectroscopy of rotational states obviously is an especially suited technique to illuminate the molecular behavior. Among them rotational tunneling spectroscopy with neutrons is the most sensitive method.^{5,6} The methyl halides have been studied systematically with this technique.^{7,8} A systematic hardening of the phonons and methyl rotational excitations was observed with reducing the size of the molecule as long as the crystal structures remain similar. Prototypically the influence of temperature and pressure on rotational tunneling systems is studied using methyl iodide.⁹ The rotational potential was found to increase with a power $n=9.6$ of decreasing interatomic distances. This large exponent reflects the importance of steric hindrance by the steep repulsive term of the intermolecular potentials. Recently the phenomenological analysis is confirmed by a description of the lattice dynamics and the single particle rotational potential based on atomic charges obtained by *ab initio* density functional theory (DFT) calculations of the isolated molecule and the intermolecular interactions and the crystal structures.¹⁰

New phenomena appear in mixed systems. Effects of local distortion fields are well known for atomic alloys. Thus it looks interesting to extend the studies of the pure materials to mixtures also in molecular alloys aiming to observe details of the global and local changes of the lattice using methyl rotational tunneling as a much more sensitive probe than ever available in atomic systems. There are already interesting investigations of solid solutions. In general only weak changes of the spectra are observed when mixing protonated and deuterated materials.¹¹ Pronounced orientational disorder has been found with diluting halo derivatives in isosteric

methyl compounds.¹² The mixed methyl halides belong to this second class of materials. Due to the simplicity of the constituents they show the phenomena in a most clear form and may thus develop into a model molecular alloy. We use rotational tunneling to study mixed methyl iodide and methyl bromide at the methyl iodide rich side with respect to local distortion fields. The structural relaxation around impurities are determined by the intermolecular interaction potentials and vice versa. Comparison with the pure materials⁷ will help to understand the observations.

II. EXPERIMENTS AND RESULTS

The pure materials were obtained from the Aldrich company. The chemical purities were better than 99.5% for both compounds. Due to the low boiling point of CH_3Br of $T_b = 4^\circ\text{C}$ the sample preparation required some care. The mixing was done in the cold room of the neutron guide hall of the ILL at a temperature of -20°C . By using cold syringes, cold sample holders, etc. the evaporation of the bromomethane during the mixing procedure was largely avoided. A handling of the samples in a room temperature environment would have required the use of cold media with a corresponding risk of contaminating the samples with water. Two samples were obtained, one with 10% of methyl bromide the second one with about 30%. The mixtures were introduced into electro-eroded flat aluminum cans of 1 mm thickness and were closed at the top flange by an indium seal. The samples were oriented in the neutron beam under 45° . The calculated scattering probability is 27%.

For interested researchers it shall be noted that this enclosure does not allow a safe long term storage of the samples. The methyl halides obviously react very slowly with the indium likely to form trimethyl indium. This compound is very sensitive to air and thus starts burning when the indium sealing leaks finally due to dissolution or if the can is opened. Due to this reaction a control of the sample composition after the experiments was not possible.

^{a)}Electronic mail: m.prager@fz-juelich.de

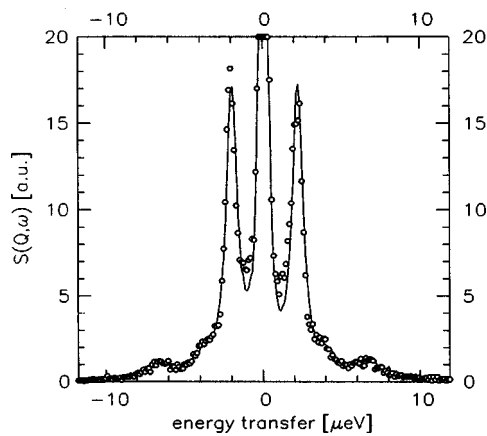


FIG. 1. Spectrum of $\text{CH}_3\text{I}_{0.9}\text{Br}_{0.1}$. Sample temperatures 2.8 K. Instrument: IN16 at ILL, polished Si(111) monochromator, $\delta E_{\text{res}} = 0.4 \mu\text{eV}$, $Q \sim 1.6 \text{ \AA}^{-1}$. Solid line: fit.

A. High-resolution neutron spectroscopy

The backscattering spectrometer IN16 of the Institut Laue Langevin, Grenoble, France, has been used.¹³ The setup with a polished Si(111) monochromator and polished Si(111) analysers allows to measure spectra in the energy window $\pm 18 \mu\text{eV}$ at an energy resolution $\delta E = 0.4 \mu\text{eV}$. Figures 1 and 2 show the spectra of the two $(\text{CH}_3\text{I})_{1-c}(\text{CH}_3\text{Br})_c$ samples at sample temperatures $T = 2.8 \text{ K}$. At low concentration $c = 0.1$ the lines are already broadened but still well resolved. Three pairs of tunneling lines can be distinguished. The dominant doublet at the lowest energy transfer is sharpest. With increasing tunnel splitting the lines get broader. At the higher concentration $c = 0.3$ the weak tunneling bands merge. A fit of individual bands can be only performed under restrictions discussed below. All fit parameters are shown in the first three lines of Table I. The tunnel splittings of the pure materials are included in the table to support the discussion.

B. Phonons

The vibrational phonon density of states (VDOS) was measured using the thermal time-of-flight spectrometer SV29 at Forschungszentrum Jülich¹⁴ at a wavelength $\lambda = 1.76 \text{ \AA}$ and an elastic energy resolution $\delta E = 2.2 \text{ meV}$ (Fig. 3). The sample temperatures were 2.2 K for both spectra. Beside changes of intensities the main features of the spectra are independent of concentration. However, lines re-

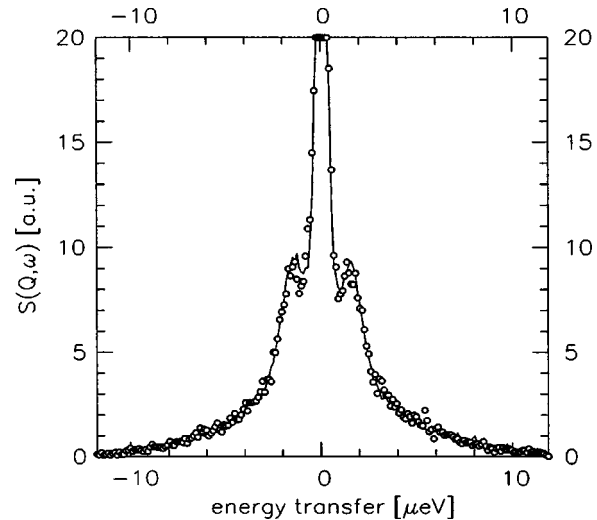


FIG. 2. Spectrum of $\text{CH}_3\text{I}_{0.7}\text{Br}_{0.3}$. Sample temperatures 2.8 K. Instrument: IN16 at ILL, polished Si(111) monochromator, $\delta E_{\text{res}} = 0.4 \mu\text{eV}$, $Q \sim 1.6 \text{ \AA}^{-1}$. Solid line: fit.

solved at $c = 0.1$ begin merging at the higher concentration. The characteristic energies are presented in Table II together with values of the pure materials taken from Ref. 7. The prominent change is the weakening and broadening of the strong doublet around 14 meV. The shoulder at $\sim 11.3 \text{ meV}$ which is not present in pure CH_3I ⁷ increases in intensity with increasing concentration of CH_3Br while the feature at 16.8 meV disappears.

III. DISCUSSION

The quantity which determines the eigenvalues of a quantum rotor is the rotational potential

$$V(\varphi) = \sum_{n=1}^N \frac{V_{3n}}{2} (1 - \cos(3n\varphi + \varphi_{3n})). \quad (1)$$

All relevant features are already contained in the case $N = 1$, a pure $\cos 3\varphi$ potential, and thus the following discussion on *changes of band energies* is restricted to this simple potential.

The one-dimensional quantum rotor is seen by neutrons via the scattering function^{5,6}

TABLE I. Tunnel splittings $\hbar\omega_t$, linewidths Γ , intensities. The elastic intensity is normalized to 1. Rotational potentials V_3 are derived from $\hbar\omega_t$. Fit parameters without errors are fixed in the fit according to the model. Occurrence probabilities of a central molecule X enclosed in a chain between two neighbors Y, Z are labeled YXZ with X, Y, Z = I or B and I = CH_3I , B = CH_3Br . Configurations BIB and BBB are not included due to their low occurrence probabilities. See the discussion.

	$c = 0.1$			$c = 0.3$			$c = 0$	$c = 1$
$\hbar\omega_t$ [μeV]	12.10 ± 0.05	3.93 ± 0.3	6.63 ± 0.2	1.58 ± 0.07	3.0	2.5	2.44	0.9
Γ [μeV]	0.26 ± 0.05	0.54 ± 0.3	0.84 ± 0.3	0.66 ± 0.06	3.0	2.5		
intensity [a.u.]	0.40 ± 0.02	0.040 ± 0.01	0.047 ± 0.01	0.29 ± 0.04	0.13	0.25	1	1
V_3 [meV]	44.0 ± 0.3	38.4 ± 0.6	33.7 ± 0.3	46.7 ± 0.4	40.5	42.4	42.2	52.2
chain sequence	III	IBI	IIB	III	IBI	IIB		
calc. occ. prob.	0.729	0.081	0.162	0.343	0.147	0.294	1	1

TABLE II. Characteristic energies of the vibrational density of states and assignment based on the knowledge of the pure materials (Ref. 7) and the model outlined in the discussion. Transverse (TA) and longitudinal (LA) acoustic phonons, methyl libration (R_z) and torsions perpendicular to the symmetry axis of the molecules ($R_{x,y}$) are assigned.

Energies [meV]						
$c=0$	4.0	7.0		13.05	14.24	17
$c=0.1$	3.8	6.6	11.3	13.1	14.3	16.8
$c=0.3$	3.8	6.6	11.3	13.4	14.3	...
$c=1$	4.8	7.9		15.7	14.5	
assignment	TA	LA	$R_z(\text{IIB})$	$R_z(\text{III})$ [$R_z(\text{BBB})$ for $c=1$]	$R_{x,y}$	

$$S_i(Q, \omega) = \left(\frac{5}{3} + \frac{4}{3}j_0(Qd)\right)\delta(\omega) + \left(\frac{2}{3} - \frac{2}{3}j_0(Qd)\right) \times \{\delta(\omega + \omega_{t_i}) + \delta(\omega - \omega_{t_i})\}. \quad (2)$$

In our simple description the only parameter of the rotational potential, V_3 , can be determined from the ground-state tunnel splitting $\hbar\omega_t$, the symmetry of the potential—in our case most likely it is threefold—from the elastic incoherent structure factor EISF via the proton proton distance d .

The presence of different tunnel transitions is a sign of the presence of multiple *well-defined environments* of the methyl groups. The tunneling spectrum in systems with N inequivalent methyl rotors is a superposition of single particle spectra $S_i(Q, \omega)$

$$S(Q, \omega) = \sum_i^N p_i S_i(Q, \omega), \quad (3)$$

with the tunnel transition energies $\hbar\omega_{t_i}$ and the occurrence probabilities p_i . Obviously $\sum p_i = 1$. According to Eq. (2) the ratio of the integrated inelastic to the purely elastic intensity is $R = (2 - 2j_0)/(5 + 4j_0)$. The inelastic intensities are near to this theoretical value. Deviations can be explained by contamination of the elastic line. Thus we assume that we have seen all tunnel transitions. In case of a binary fully miscible alloy disorder increases with the concentration approaching 0.5. In agreement with this rule sharp structures are found mainly at low concentration.

A first straightforward assignment would try to distinguish methyl rotors by the type of molecule and on the basis of the tunnel splittings of the pure compounds. The strongest transition is indeed near to the tunnel splitting of pure methyl iodide. This strong line unfortunately hides the energy range of the tunnel splitting of pure methyl bromide. However, the presence of two further tunneling lines of comparable intensities but at higher energy transfers tells us that this approach is too simple. Therefore, we take into account in a next refined model the local environment of the molecules. The building units of the crystal structure are chains of antiparallelly oriented dipoles.^{15,16} The essential feature is contained in this isolated chain. We distinguish four characteristic environments. A CH_3I enclosed between two other CH_3I molecules we abbreviate as III, CH_3Br enclosed between two CH_3I as IBI, CH_3I enclosed between one CH_3I and one CH_3Br as IIB and finally a CH_3Br enclosed between one CH_3I and one

CH_3Br as IBB. The statistical occurrence probabilities for the four species are shown in the last line of Table I for the two concentrations used.

With the relative intensities of line 3 of Table I the strongest peak must be assigned to a methyl iodide enclosed between two similar molecules. The tunnel frequency is smaller than in pure methyl iodide which is typical of an increased rotational barrier. The contraction of the average lattice parameter due to the presence of the smaller methyl bromide molecules can be qualitatively identified as the source of this shift.

In a semiquantitative model the lattice parameters of a binary compound follows in general from those of the two pure constituents at a same temperature^{15,16} by Vegard's law, a linear dependence of r on the concentration. The rotational potential varies with a power n of the distance. This way we have

$$r(c) = (1 - c * 0.0526) * r(0), \quad (4)$$

$$V_{\text{rot}}(c) = V(r(0)) \left(\frac{r(0)}{r(c)} \right)^n.$$

The exponent n mirrors the r -dependence of the effective intermolecular interaction potentials. The first nonvanishing multipole moment of a methyl group is an octupole moment. For an electrostatic octupole–monopole interaction $n=4$ is calculated. The increase of the strength of the rotational potential V_{rot} of the III configuration with concentration (values of Table I) is rather well reproduced by an exponent $n=7$. This larger value shows the importance of steric hindrance by the repulsive term of a Lennard-Jones potential.

In methyl iodide under pressure a stronger r -dependence of the rotational potential is found, $n=9.6$.⁹ If we accept that this exponent characterizes still the interaction between methyl iodide molecule in the alloy then the observed smaller exponent must be due to local deviations of intermolecular distances from Vegard's law. Indeed, the microscopic inhomogeneity of a solid solution leads to relaxation of the lattice around a guest, in our case a CH_3Br molecule, the so called distortion field. We estimate the relaxation around the defect by requiring that the exponent $n=9.6$ applied to the relaxed structure has the same effect as the measured exponent $n=7$ to a homogeneous system: $(r(c)/r(0))_{\text{unrelaxed}}^7 = (r(c)/r(0))_{\text{relaxed}}^{9.6}$. The numerical evaluation shows that the relative reduction of the local molecular displacement

between two neighboring CH_3I molecules is by 1.3% smaller than postulated from Vegard's law. Since Eq. (4) is valid globally their must be a relaxation of CH_3Br molecules towards CH_3I to maintain the overall compression. We will see below that this requirement fits well to our observation.

It must be admitted that the relaxation also involves angular degrees of freedom and it may be a rotation of the molecule which reduces to close approaches. It is further worth to notice that due to the random distribution of guest molecules in solid solutions such changes are not accessible to diffraction techniques. Tunneling spectroscopy is a unique probe of weak local disorder.

From their intensity the line at $3.93 \mu\text{eV}$ is assigned to isolated methyl bromide molecules (IBI). Such a remarkable shift by a factor 4.4 compared to pure CH_3Br with $\hbar\omega_t = 0.9 \mu\text{eV}$ follows precisely from our model, however. Since the estimate is based on pure CH_3Br the important quantity is now the concentration of methyl iodide and Eq. (4) has to be applied with $c^* = 1 - c = 0.9$. If one scales the rotational potential and the tunnel splitting of pure CH_3Br by the increased interatomic distances and the power $n=7$ of the interaction potential obtained above for the III configuration one gets very close to the observed tunneling splitting. The parameters are shown in Table I.

Based on the occurrence probabilities the third tunneling transition at $6.63 \mu\text{eV}$ can only be assigned to methyl groups of CH_3I facing a minority CH_3Br molecule. In this case the argumentation within our simple model cannot be such quantitative since two counteracting effects have to be taken into account. On the one hand the global lattice contraction requires a reduction of the tunnel splitting. On the other hand the small CH_3Br neighbor creates free volume around the CH_3I molecule and allows it to minimize its energy by displacing towards the guest molecule. The observed increase of the tunnel splitting shows that this second influence is dominant. Quantitatively the increase of the tunnel splitting by the factor 2.6 compared to pure CH_3I is equivalent to a reduction of the barrier to rotation by about 5%. If the smaller size of CH_3Br would fully contribute to a local increase of interatomic distances we would have to apply our model $c=1$ starting from the reduced lattice parameter $r(c=0.1)$. We obtain $V_3^{\text{calc}} = 31.3 \text{ meV}$ with tunnel splitting of $8.8 \mu\text{eV}$. The difference must be again attributed to local relaxation. From the relation $V_3^{\text{calc}}/V_3^{\text{obs}} = 31.3/33.7 = (1-x)^7$ we get the relative change x of this relaxation. $x = 1.1\%$ is very close and consistent to the estimate from the main tunneling peak (see above). A fully quantitative mathematical treatment based on energy minimized mixed clusters of molecules will not improve the understanding of the phenomena and is beyond the scope of this paper.

At the higher concentration the individual bands merge into a broad inelastic intensity. Its maximum has shifted to lower energy transfers. Within our model (Vegard's law and $n=7$) this shift follows quantitatively if the CH_3Br concentration of the sample would have been $c=0.28$. This reduced compared to the nominal concentration of $c=0.3$ is within the accuracy of the sample preparation process which involves the risk of loosing some of the more volatile CH_3Br . It is impossible to fit the other features of the spectrum by

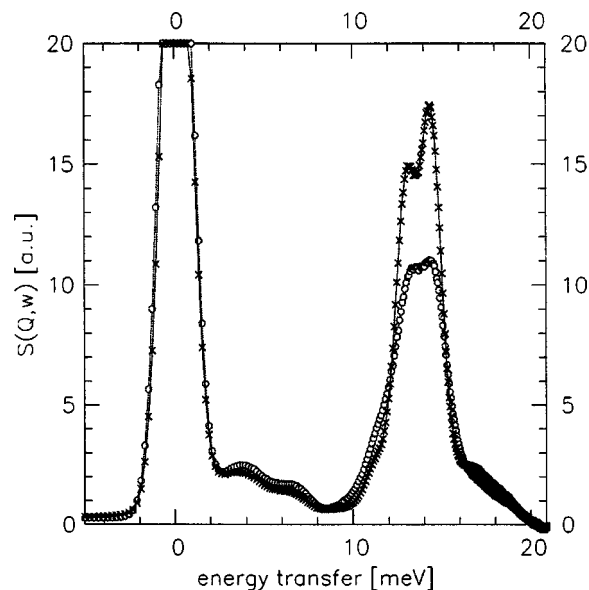


FIG. 3. Vibrational density of states of $\text{CH}_3\text{I}_{1-x}\text{Br}_x$. Sample temperatures 2.2 K. $c=0.1$ (○) and $c=0.3$ (×). Sample temperature 2.2 K. Spectrometer SV29, FZJ, $\lambda=1.76 \text{ \AA}$.

independent parameters. Based on our model we have fixed the relative line intensities and the position of the weakest line according to the model. The final fit is shown in Fig. 2 and reproduces well the measured spectrum. While this consistency supports our interpretation it is, due to the imposed restrictions, not an independent proof.

The VDOS (Fig. 3) contains a shoulder at the low energy side of the dominant double peak which is not present in the pure CH_3I .⁷ This shoulder gets more weight with increasing concentration of CH_3Br . Two methyl librational bands are due to or strongly influenced by the guest molecules, the librations R_z of the methyl groups of CH_3Br and those of CH_3I neighboring a bromide guest. From the observed tunneling transitions we can estimate the librational energies. A limitation to pure $\cos(3\varphi)$ potentials can in general not give an exact description of both excitations. But this simplest of all rotational potentials allows already a good guess of relative shifts. For CH_3Br in the configuration IBI the shift towards lower energies compared to the pure compound is estimated to be about 2.5 meV, for CH_3I in the configuration IIB a 1.7 meV shift is expected. This means that in very good agreement with its position the new band at 11.3 meV must be assigned to matrix CH_3I molecules facing a CH_3Br guest molecule while the CH_3Br librational modes coincides with the strong methyl librational band of almost unperturbed CH_3I molecules (Table II).

IV. CONCLUSION

Methyl iodide and methyl bromide form solid solutions. At bromide concentrations $c < 0.3$ the global and local distortion is studied using methyl rotational tunneling as sensitive probe. The mean contraction of the lattice with increasing c is found to be responsible of an increase of the

rotational barrier of the majority component CH_3I in an environment of same molecules. The rotational potential increases with the reduction of the mean intermolecular distance proportional to r^{-7} . A relaxation of the methyl iodide molecules facing a guest molecule by 1.3% towards the smaller guest molecules explains the deviation from the r -dependence $r^{-9.6}$ of the rotational potential found in a pressure experiment on CH_3I .⁹ The increased distance to matrix molecules and the r^{-7} -dependence of the rotational potential also explains quantitatively the reduction of the rotational barrier of isolated CH_3Br molecules. A special consideration requires a CH_3I matrix molecule facing a CH_3Br defect. The combined action of global contraction and local free volume leads to a weakening of the rotational potential. Again a relaxation by 1.3% describes the observed shift of the tunneling mode nicely.

Applying the same ideas to the case of CH_3I guests in a CH_3Br matrix makes us expect a strongly compressed tunneling spectrum with all transition energies merged below $1.1 \mu\text{eV}$. A neutron scattering experiment will thus be unable to distinguish the individual molecular species at the CH_3Br side of the CH_3I – CH_3Br phase diagram.

ACKNOWLEDGMENT

I thank T. Seydel for the help with the experiment and the Institut Laue Langevin for the beamtime.

- ¹I. Silvera, Progress Reports in Physics 1980.
- ²Y. Ozaki, Y. Kataoka, and T. Yamamoto, J. Chem. Phys. **73**, 3442 (1980).
- ³COMP Programming, Fall 1999 National meeting, New Orleans 1999, *Quantum Simulations of Complex Many-Body Systems: From Theory to Algorithms*, edited by J. Grotendorst, D. Marx, and A. Muramatsu, NIC Series, Vol. 10, ISBN 3-00-009057-6, Jülich 2002.
- ⁴A. Anderson, B. Andrews, and B. H. Torrie, J. Chim. Phys. **82**, 99 (1985).
- ⁵W. Press, *Single Particle Rotations in Molecular Crystals, Springer Tracts in Modern Physics, Vol. 81* (Springer, Berlin, 1981).
- ⁶M. Prager and A. Heidemann, Chem. Rev. **97**, 2933 (1997).
- ⁷M. Prager, J. Stanislawski, and W. Häusler, J. Chem. Phys. **86**, 2563 (1987).
- ⁸M. Prager, J. Chem. Phys. **89**, 1181 (1988).
- ⁹M. Prager, C. Vettier, and S. Mahling-Ennanoui, Z. Phys. B: Condens. Matter **75**, 217 (1989).
- ¹⁰O. Kirstein and M. Prager, J. Chem. Phys. (to be published).
- ¹¹D. Cavagnat, S. F. Trevino, and A. Magerl, J. Phys.: Condens. Matter **1**, 1047 (1989).
- ¹²M. Prager, P. Schiebel, and J. Combet, Chem. Phys. **276**, 69 (2002).
- ¹³<http://www.ill.fr/>
- ¹⁴M. Prager, Physica B **283**, 376 (2000); and http://www.fz-juelich.de/iff/Institute/ins/Broschuere_NSE/sv29.shtml
- ¹⁵T. Kawaguchi, M. Hijikigawa, Y. Hayafuji, M. Ikeda, R. Fukushima, and Y. Tomie, Bull. Chem. Soc. Jpn. **46**, 53 (1973).
- ¹⁶P. Gerlach, B. H. Torrie, and B. M. Powell, Mol. Phys. **57**, 919 (1986).